Shock and Vibration 13 (2006) 197–214
IOS Press

Dynamic stability of a circular pre-stressed elastic orthotropic plate subjected to shock excitation

Yuriy A. Rossikhin and Marina V. Shitikova*
Department of Theoretical Mechanics, Voronezh State University of Architecture and Civil Engineering, ul. Svobodu 45-53, Voronezh 394018, Russia

Dedicated to the 75th Birthday of our teacher Professor Duis D. Ivlev

Received 19 September 2005
Revised 8 November 2005

Abstract. The problem on low-velocity impact of an elastic body upon a pre-stressed circular orthotropic plate possessing cylindrical anisotropy is considered. The dynamic behavior of the plate is described by equations taking the rotary inertia and transverse shear deformations into account. Longitudinal compressing forces are uniformly distributed along the plate's median plane. Contact interaction is modeled by a linear spring, and a force arising in it is the linear approximation of Herts'z contact force. During the shock interaction of the impactor with the plate, the waves which are the surfaces of strong discontinuity are generated in the plate and begin to propagate. Behind the fronts of these waves, the solution is constructed in terms of ray series, which coefficients are the different order discontinuities in partial time-derivatives of the desired functions, and a variable is the time elapsed after the wave arrival at the plate's point under consideration. The ray series coefficients are determined from recurrent equations within accuracy of arbitrary constants, which are then determined from the conditions of dynamic contact interaction of the impactor with the target. The found arbitrary constants allow one to construct the solution both within and out of the contact region. The analysis of the solution obtained enables one to find out the new effect and to make the inference that under a certain critical magnitude of the compression force the orthotropic plate goes over into the critical state, what is characterized by 'locking' the shear wave within the contact region, resulting in plate damage within this zone as soon as the compression force exceeds its critical value.

Keywords: Ray method, dynamic stability, shock interaction, elastic orthotropic plate, initial stresses

1. Introduction

During the past two decades foreign object impact damage to composite structures has received a great deal of attention, since laminated fiber-reinforced composite plates are known to be susceptible to damage resulting from accidental impact by foreign objects [5–8,11–13,20–23,26]. Impact on aircraft structures or civil engineering structures, for instance, from dropped tools, hail, and debris thrown up from the runway, poses a problem of great concern to designers. Since the impact response is not purely a function of material's properties and depends also on the dynamic structural behavior of the composite plate, it is important to have a basic understanding of the structural response and how it is affected by different parameters [11]. From this point of view, analytical models are useful as they allow systematic parametric investigation and provide a foundation for prediction of impact damage.

*Corresponding author. Tel./Fax: +07 4732 773992; E-mail: shitikova@vmail.ru.

ISSN 1070-9622/06/$17.00

A large number of studies have been performed on the effect of impact loading on composites and have been reviewed in [1–3]. Although many important contribution have been made to numerical analysis of the impact response of composite plates, the corresponding analytical solutions are very few [1–3,11,12,16,22].

An impact response analysis requires a good estimate of contact force throughout the impact duration. Low-velocity impact problems, which also took the local indentation into account, have been solved by many authors. Reference to the state-of-the-art papers [1,2] shows that in most studies it was assumed that the impacted structure was free of any initial stresses. But this does not adequately reflect the real multidirectional complex loading states that the materials experience during their service life. In practice, the composite facing of a structure may be under a preload, e.g., a sandwich structure with laminate facing under bending loads, jet engine fan blades subjected to centrifugal forces [20]. Even when stationary on the runway a composite airframe is under pre-stress [26]. The other example of great practical interest is the analysis of impact response of pipes pressurised for hydro-tests subjected to dropped tools [13].

Very few works have reported on the impact response of anisotropic and composite plates and beams subjected to an initial uniaxially preloading [5,8,20,21], as well as biaxial preloading [6,7,13,22,23,26].

Sun and Chattopadhyay [22] investigated dynamic response of rectangular anisotropic laminated plates under initial tensile stress to impact of a mass. The equations of plate motion take the transverse shear deformations into account, but ignore the rotary inertia of a normal in the direction of coordinate axes lying in the plate's median plane [25]. For the effect of local deformation at the point of contact, the Hertz law is assumed, but out of the contact region impact interaction results in vibratory motion of the plate. As a result, the Timoshenko type nonlinear integral equation for the contact force is written, which is further solved numerically by means of small-time increment method. It is found that a higher initial tensile stress elevates the maximum contact force, but reduces the contact time, the deflection, and the stresses, and increases the velocity of disturbance propagation, i.e., the effect of dynamic strengthening of the plate material is observed.

Finite element method was used in [20] to study the impact response of a graphite-epoxy laminated beam for various combinations of impact velocities and preloads. The contact force was assumed to be proportional to the squared value of the local indentation. It has been reported that the tensile initial stresses reduce the impact duration, but the maximum impact force is not very much affected by the preload. From the experiments carried out and presented in [21] for varifying numerical calculations of [20] it was found that tensile initial stresses reduce the threshold impact velocity for damage, but beyond certain impact velocity they may help in containing delamination.

When investigating dynamic large deflection response of prestressed composite laminates subjected to impact [6] using the finite element method, it is found that initial tensile stress tends to intensify the contact force while reducing the contact time, and an opposite conclusion is obtained for initial compressive stress. It is noted that initial compressive stress may result in larger deflection amplitudes.

Problems on stability of rigid bodies with respect to nonstationary excitations are of great practical consequence as well. However, their analysis still presents severe mathematical difficulties, and particularly this concerns to the problems dealing with shock excitations on rigid bodies.

The problem on the dynamic stability of an infinite plate of constant thickness resting on an elastic foundation with respect to nonstationary excitation was first considered in [14]. An anisotropic elastic half-space with an absolutely smooth boundary was used as the foundation, such that friction between the plate and the half-space boundary was absent. It was assumed also that tangential and normal forces acted in the plate mid-plane. The dynamic behavior of the plate was described by the classical Kirchhoff-Love equation. Nonstationary vibrations were excited by snap-action loads, resulting in three types of plane shock waves propagating in the elastic anisotropic half-space. The solution behind the wavefronts up to the contact boundary was constructed by using ray series. Coefficients of the ray series, within an accuracy of arbitrary functions dependent on two coordinates on the plate mid-plane, were determined from recurrent differential equations of the ray method, which had been derived from the system of equations describing the dynamic behavior of the anisotropic half-space using the theory of discontinuities [24]. Arbitrary functions, in their turn, were found from the condition of absence of tangential stresses and the condition of continuity for normal displacements and normal stresses on the contact boundary of the plate and the half-space, as well as from the initial conditions. The time-dependence and the mid-plane coordinates dependence of the plate deflection were obtained as a result of calculations. It was shown that the behavior of the plate deflection with time is dependent on the values of the compression force involved in the plate mid-plane. If these values exceeded the

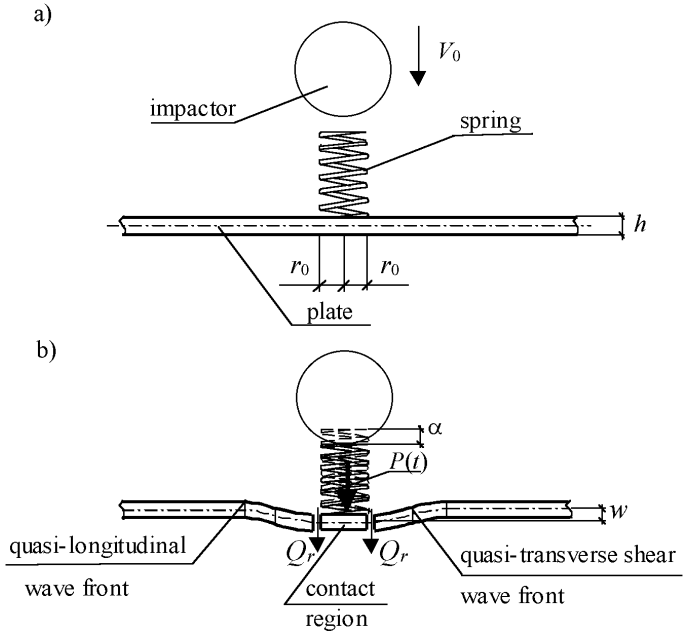

Fig. 1. Scheme of the shock interaction of an impactor with a plate: (a) before impact, and (b) after impact.

critical values (these critical values were less than the critical values of the compression forces under which the plane form of equilibrium of the plate became unstable), then the normal displacements of some set of points possessed by the plate might take on rather large values in a small instant of the time.

In an identical way and using the same method, Rossikhin and Shitikova [15,17] have solved the problem of dynamic stability of an elastic transversely isotropic plate being in welded or smooth contact with an elastic isotropic half-space. Stability analysis has been performed for two types of the plate: a relatively heavy and rigid plate and a relatively lightweight and complaint plate with respect to the half-space material.

In the present paper, the low-velocity impact response of a circular pre-stressed elastic orthotropic plate possessing curvilinear anisotropy is investigated. The equations of plate motion take the rotary inertia and transverse shear deformations into account. Contact interaction is modeled by a linear spring, and a force arising in it is the linear approximation of Herts'z contact force. Stability or instability of the plate is established by analyzing the behavior of transient waves generating in the plate at the moment of impact, which further propagate along its median surface as 'diverging circles'.

2. Problem formulation and governing equations

Assume an elastic body of the mass m impacts a circular pre-stressed orthotropic plate of the thickness h with the velocity V_0. The plate is presumed to be of infinite extent in order to ignore the waves reflected from its edges. Contact interaction is modeled by a linear elastic circular spring of the radius r_0, which lower end is embedded into the plate (Fig. 1a). The force arising in the spring is connected with the magnitude of its compression $\alpha - w$ by the following relationship:

$$P(t) = E_1(\alpha - w) \tag{1}$$

where E_1 is the stiffness coefficient of the spring, α is the displacement of the spring's upper end, and w is the displacement of its lower end, which is equal to the plate deflection at the point of contact (Fig. 1b).

A linear spring acting between the impactor and the plate centerline deflection was also used in [12] to represent the linearized Hertzian contact deformation during the impact response analysis of a rectangular orthotropic plate, when its dynamic motion is described by the equations developed in [25]. Based on Laplace transform techniques, a

closed-form solution is obtained for simply supported plate free from initial stresses. The solution obtained has been compared with that of the similar problem involving nonlinear Hertzian contact. In the second case, the solution technique is based on a Rayleigh-Ritz approach with numerical integration in time. As calculations show, the results according to these two approaches for the relatively thin plates are essentially the same for calculated impact forces and strains behind the impact point.

The motion of the impactor during its contact with the target is described by the equation

$$m\ddot{y} = -P(t) \tag{2}$$

and the equation of motion of the contact region as a rigid whole has the form

$$M\dot{W} = 2\pi r_0 Q_r|_{r=r_0} + P(t) \tag{3}$$

where an overdot denotes a derivative with respect to time t, $y = \alpha + w$ is the total displacement of the impactor, $W = \dot{w}$, M is the mass of the contact spot, and Q_r is the transverse force on the area with the r-normal.

Aside from Eqs (2) and (3), the continuity condition for tangent of the angle of the slope of the tangent to the w-curve on the contact region boundary should be fulfilled

$$\frac{\partial w}{\partial r}\Big|_{r=r_0} = 0 \tag{4}$$

The initial conditions

$$W|_{t=0} = 0, \qquad \dot{\alpha}|_{t=0} = V_0 \tag{5}$$

as well as the equations of motion of the plate should be added to Eqs (1)–(4).

As further an axially symmetric problem is considered, and the rotary inertia of the normal to the plate in the r-axis direction and transverse shear deformation dominate during impact process, then equations of motion of the elastic orthotropic plate are written in the form (see Appendix A)

$$D_r\left(\frac{\partial^2\varphi}{\partial r^2} + \frac{1}{r}\,\frac{\partial\varphi}{\partial r}\right) - D_\theta\,\frac{\varphi}{r^2} + hKG_{rz}\left(\frac{\partial w}{\partial r} - \varphi\right) = \rho\,\frac{h^3}{12}\,\ddot{\varphi} \tag{6}$$

$$KG_{rz}\left(\frac{\partial^2 w}{\partial r^2} - \frac{\partial\varphi}{\partial r} + \frac{1}{r}\,\frac{\partial w}{\partial r} - \frac{\varphi}{r}\right) = \rho\ddot{w} + \frac{N}{h}\,\Delta w \tag{7}$$

where N is the constant compression force acting in the radial direction,

$$\Delta = \frac{1}{r}\,\frac{\partial}{\partial r}\left(r\,\frac{\partial}{\partial r}\right)$$

and other values are defined in Appendix A. The origin of the polar coordinate system is located at the center of the plate, i.e. at the center of the contact region.

For the isotropic case $D_r = D_\theta$, and Eqs (6) and (7) go over into equations investigated in [9].

3. Recurrent equations of the ray method

It is assumed that as a result of impact upon the plate, the surfaces of strong discontinuity arise in it on the boundary of the contact region $r = r_0$, which further propagate along the plate in the form of diverging cylindrical surfaces-strips.

The solution behind the wave front of strong discontinuity Σ is constructed in terms of the ray series [18]

$$Z(r,t) = \sum_{k=0}^{\infty}\frac{1}{k!}\,[Z_{,(k)}]_{t=(r-r_0)/G}\left(t - \frac{r-r_0}{G}\right)^k H\left(t - \frac{r-r_0}{G}\right) \tag{8}$$

where Z is the function to be determined, $Z_{,(k)} = \partial^k Z/\partial t^k$, $[Z_{,(k)}] = Z^+_{,(k)} - Z^-_{,(k)}$, the signs "+" and "−" refer to the magnitudes of the derivative in $Z_{,(k)}$ calculated before and behind the wave surface Σ, respectively, G is the normal velocity of the wave Σ, and $H\left(t - (r-r_0)G^{-1}\right)$ is the unit Heaviside function.

To determine the coefficients of the ray series (8) for the desired function Z, it is necessary to differentiate the governing Eqs (6) and (7) for the plate k times with respect to time, take their difference on the different sides of the wave surface, and apply the condition of continuity for the physical components of the values to be found [19]

$$G^n\left[\frac{\partial^n Z_{,(k)}}{\partial r^n}\right]=\sum_{m=0}^{n}(-1)^m\,\frac{n(n-1)\dots(n-m+1)}{m!}\,\frac{\delta^{n-m}[Z_{,(k+m)}]}{\delta t^{n-m}} \tag{9}$$

where $\delta/\delta t$ is the δ-derivative with respect to time [24].

As a result of such a procedure, we are led to a set of recurrent equations of the ray method

$$\left(1-\frac{\rho G^2}{B_r}\right)\omega_{(k+1)}=2\,\frac{\delta\omega_{(k)}}{\delta t}+Gr^{-1}\omega_{(k)}+b_rGX_{(k)}+F_{1(k-1)} \tag{10}$$

$$\left(1-\frac{\rho G^2+Nh^{-1}}{KG_{rz}}\right)X_{(k+1)}=2a\,\frac{\delta X_{(k)}}{\delta t}+Gr^{-1}aX_{(k)}-G\omega_{(k)}+F_{2(k-1)} \tag{11}$$

where

$$X_{(k)}=[w_{,(k+1)}],\quad \omega_{(k)}=[\varphi_{,(k+1)}],\quad r=r_0+Gt$$

$$b_r=12Kh^{-2}G_{rz}B_r^{-1},\quad a=1-N(hKG_{rz})^{-1}$$

$$F_{1(k-1)}=-\frac{\delta^2\omega_{(k-1)}}{\delta t^2}-Gr^{-1}\,\frac{\delta\omega_{(k-1)}}{\delta t}+G^{-2}r^{-2}\,\frac{E_\theta}{E_r}\,\omega_{(k-1)}-b_rG\,\frac{\delta X_{(k-1)}}{\delta t}+b_rG^2\omega_{(k-1)}$$

$$F_{2(k-1)}=-a\,\frac{\delta^2X_{(k-1)}}{\delta t^2}-Gr^{-1}a\,\frac{\delta X_{(k-1)}}{\delta t}+G\,\frac{\delta\omega_{(k-1)}}{\delta t}+G^2r^{-1}\omega_{(k-1)}$$

Putting $k=-1,0,1,2,\dots$ in Eqs (10) and (11) yields on the first wave

$$\rho{G^{(1)}}^2=B_r,\quad \omega_{(0)}^{(1)}=c_0^{(1)}r_1^{-1/2},\quad X_{(0)}^{(1)}=0,\quad X_{(1)}^{(1)}=-\frac{1}{af_r}\,G^{(1)}c_0^{(1)}r_1^{-1/2}$$

$$\omega_{(1)}^{(1)}=c_1^{(1)}r_1^{-1/2}+\frac{1}{2}\left(\frac{E_\theta}{E_r}-\frac{1}{4}\right)G^{(1)}c_0^{(1)}r_1^{-3/2}+\frac{1}{2}\,b_r\left(\frac{1}{af_r}-1\right)G^{(1)}c_0^{(1)}r_1^{1/2}$$

$$X_{(2)}^{(1)}=-\frac{G^{(1)}}{af_r}\left[c_1^{(1)}r_1^{-1/2}+\frac{1}{2}\left(\frac{E_\theta}{E_r}-\frac{5}{4}\right)G^{(1)}c_0^{(1)}r_1^{-3/2}+\frac{1}{2}\,b_r\left(\frac{1}{af_r}-1\right)G^{(1)}c_0^{(1)}r_1^{1/2}\right]$$

$$\begin{aligned}\omega_{(2)}^{(1)}=&\,c_2^{(1)}r_1^{-1/2}+\frac{1}{2}\left(\frac{E_\theta}{E_r}-\frac{1}{4}\right)G^{(1)}c_1^{(1)}r_1^{-3/2}+\frac{1}{2}\,b_r\left(\frac{1}{af_r}-1\right)G^{(1)}c_1^{(1)}r_1^{1/2}\\&+\frac{1}{8}\left(\frac{E_\theta}{E_r}-\frac{1}{4}\right)\left(\frac{E_\theta}{E_r}-\frac{9}{4}\right){G^{(1)}}^2c_0^{(1)}r_1^{-5/2}+\frac{1}{8}\,b_r^2\left(\frac{1}{af_r}-1\right)^2{G^{(1)}}^2c_0^{(1)}r_1^{3/2}\end{aligned}$$

$$\begin{aligned}X_{(3)}^{(1)}=&-\frac{G^{(1)}}{af_r}\left[c_2^{(1)}r_1^{-1/2}+\frac{1}{2}\left(\frac{E_\theta}{E_r}-\frac{5}{4}\right)G^{(1)}c_1^{(1)}r_1^{-3/2}+\frac{1}{2}\,b_r\left(\frac{1}{af_r}-1\right)G^{(1)}c_1^{(1)}r_1^{1/2}\right.\\&+\frac{1}{8}\,b_r^2\left(\frac{1}{af_r}-1\right)^2{G^{(1)}}^2c_0^{(1)}r_1^{3/2}+b_r\left(\frac{1}{af_r}-1\right)\left(\frac{1}{f_r}-\frac{3}{4}\right){G^{(1)}}^2c_0^{(1)}r_1^{-1/2}\\&\left.+\frac{1}{8}\left(\frac{E_\theta}{E_r}-\frac{1}{4}\right)^2{G^{(1)}}^2c_0^{(1)}r_1^{-5/2}-\frac{1}{f_r}\left(\frac{E_\theta}{E_r}-1\right){G^{(1)}}^2c_0^{(1)}r_1^{-5/2}\right]\end{aligned} \tag{12}$$

$$\omega_{(3)}^{(1)} = c_3^{(1)} r_1^{-1/2} + \frac{1}{2}\left(\frac{E_\theta}{E_r} - \frac{1}{4}\right) G^{(1)} c_2^{(1)} r_1^{-3/2} + \frac{1}{2}\, b_r \left(\frac{1}{af_r} - 1\right) G^{(1)} c_2^{(1)} r_1^{1/2}$$
$$+\frac{1}{8}\left(\frac{E_\theta}{E_r} - \frac{1}{4}\right)\left(\frac{E_\theta}{E_r} - \frac{9}{4}\right) {G^{(1)}}^2 c_1^{(1)} r_1^{-5/2} + \frac{1}{8}\, b_r^2 \left(\frac{1}{af_r} - 1\right)^2 {G^{(1)}}^2 c_1^{(1)} r_1^{3/2}$$
$$+\frac{1}{48}\left(\frac{E_\theta}{E_r} - \frac{1}{4}\right)\left(\frac{E_\theta}{E_r} - \frac{9}{4}\right)\left(\frac{E_\theta}{E_r} - \frac{25}{4}\right) {G^{(1)}}^3 c_0^{(1)} r_1^{-7/2}$$
$$-\frac{1}{2}\,\frac{b_r}{af_r}\left(\frac{E_\theta}{E_r} - 1\right)\left(\frac{3}{4} - \frac{1}{f_r}\right) {G^{(1)}}^3 c_0^{(1)} r_1^{-3/2} + \frac{1}{2}\,\frac{b_r}{af_r}\left(\frac{1}{af_r} - 1\right)\left(\frac{1}{f_r} - 1\right) {G^{(1)}}^3 c_0^{(1)} r_1^{1/2}$$
$$-\frac{1}{16}\, b_r \left(\frac{1}{af_r} - 1\right)\left[\left(\frac{E_\theta}{E_r} - \frac{1}{4}\right)^2 - \frac{3}{2} - \left(\frac{E_\theta}{E_r} - \frac{1}{4}\right)\left(\frac{E_\theta}{E_r} - \frac{9}{4}\right) af_r\right] {G^{(1)}}^3 c_0^{(1)} r_1^{-3/2}$$
$$-\frac{1}{16}\, b_r^2 \left(\frac{1}{af_r} - 1\right)^2 \left(\frac{E_\theta}{E_r} - \frac{9}{4}\right) {G^{(1)}}^3 c_0^{(1)} r_1^{1/2} + \frac{1}{48}\, b_r^3 \left(\frac{1}{af_r} - 1\right)^3 {G^{(1)}}^3 c_0^{(1)} r_1^{5/2}$$

and on the second wave

$$\rho {G^{(2)}}^2 = aKG_{rz}, \quad \omega_{(0)}^{(2)} = 0, \quad X_{(0)}^{(2)} = c_0^{(2)} r_2^{-1/2}, \quad \omega_{(1)}^{(2)} = \frac{b_r}{e_r}\, G^{(2)} c_0^{(2)} r_2^{-1/2}$$

$$X_{(1)}^{(2)} = c_1^{(2)} r_2^{-1/2} - \frac{1}{8}\, G^{(2)} c_0^{(2)} r_2^{-3/2} + \frac{1}{2}\,\frac{b_r}{ae_r}\, G^{(2)} c_0^{(2)} r_2^{1/2}$$

$$\omega_{(2)}^{(2)} = \frac{b_r}{e_r}\, G^{(2)} \left(c_1^{(2)} r_2^{-1/2} + \frac{3}{8}\, G^{(2)} c_0^{(2)} r_2^{-3/2} + \frac{1}{2}\,\frac{b_r}{ae_r}\, G^{(2)} c_0^{(2)} r_2^{1/2}\right)$$

$$X_{(2)}^{(2)} = c_2^{(2)} r_2^{-1/2} - \frac{1}{8}\, G^{(2)} c_1^{(2)} r_2^{-3/2} + \frac{1}{2}\,\frac{b_r}{ae_r}\, G^{(2)} c_1^{(2)} r_2^{1/2}$$
$$+\frac{9}{128}\, {G^{(2)}}^2 c_0^{(2)} r_2^{-5/2} + \frac{1}{8}\,\frac{b_r^2}{a^2 e_r^2}\, {G^{(2)}}^2 c_0^{(2)} r_2^{3/2}$$

$$\omega_{(3)}^{(2)} = \frac{b_r}{e_r}\, G^{(2)} \left[c_2^{(2)} r_2^{-1/2} + \frac{3}{8}\, G^{(2)} c_1^{(2)} r_2^{-3/2} + \frac{1}{2}\,\frac{b_r}{ae_r}\, G^{(2)} c_1^{(2)} r_2^{1/2}\right.$$
$$+\frac{1}{e_r}\left(\frac{E_\theta}{E_r} - 1\right) {G^{(2)}}^2 c_0^{(2)} r_2^{-5/2} - \frac{15}{128}\, {G^{(2)}}^2 c_0^{(2)} r_2^{-5/2} - \frac{1}{4}\,\frac{b_r^2}{ae_r}\, {G^{(2)}}^2 c_0^{(2)} r_2^{-1/2} \qquad (13)$$
$$\left.+\frac{b_r^2}{e_r}\left(\frac{1}{ae_r} + 1\right) {G^{(2)}}^2 c_0^{(2)} r_2^{-1/2} + \frac{1}{8}\,\frac{b_r^2}{a^2 e_r^2}\, {G^{(2)}}^2 c_0^{(2)} r_2^{3/2}\right]$$

$$X_{(3)}^{(2)} = c_3^{(2)} r_2^{-1/2} - \frac{1}{8}\, G^{(2)} c_2^{(2)} r_2^{-3/2} + \frac{1}{2}\,\frac{b_r}{ae_r}\, G^{(2)} c_2^{(2)} r_2^{1/2} + \frac{9}{128}\, {G^{(2)}}^2 c_1^{(2)} r_2^{-5/2}$$
$$+\frac{1}{8}\,\frac{b_r^2}{a^2 e_r^2}\, {G^{(2)}}^2 c_1^{(2)} r_2^{3/2} - \frac{75}{1024}\, {G^{(2)}}^3 c_0^{(2)} r_2^{-7/2} - \frac{1}{2}\,\frac{b_r}{ae_r^2}\left(\frac{E_\theta}{E_r} - 1\right) {G^{(2)}}^3 c_0^{(2)} r_2^{-3/2}$$
$$-\frac{9}{256}\,\frac{b_r}{ae_r}\, {G^{(2)}}^3 c_0^{(2)} r_2^{-3/2} + \frac{1}{2}\,\frac{b_r^2}{ae_r^2}\left(\frac{1}{ae_r} + 1\right) {G^{(2)}}^3 c_0^{(2)} r_2^{1/2} - \frac{23}{64}\,\frac{b_r^2}{a^2 e_r^2}\, {G^{(2)}}^3 c_0^{(2)} r_2^{1/2}$$
$$+\frac{1}{48}\,\frac{b_r^3}{a^3 e_r^3}\, {G^{(2)}}^3 c_0^{(2)} r_2^{5/2}$$

where $r_\alpha = r_0 + G^{(\alpha)} t \quad (\alpha = 1, 2)$, $c_i^{(\alpha)} \quad (i = 0, 1, 2, 3)$, $\quad (\alpha = 1, 2)$ are arbitrary constants,

$$f_r = 1 - \frac{G^{(1)^2}}{G^{(2)^2}}, \quad e_r = 1 - \frac{G^{(2)^2}}{G^{(1)^2}}$$

The found discontinuities $\omega_{(i)}^{(\alpha)}$ and $X_{(i)}^{(\alpha)}$ $(i = 0, 1, 2, 3),$ $(\alpha = 1, 2)$ allow one on the basis of the ray series (8) to write the expressions for the desired functions W and Q_r in terms of the truncated ray series

$$W = \sum_{\alpha=1}^{2} \sum_{k=0}^{4} \frac{1}{k!} X_{(k)}^{(\alpha)}\Big|_{y_\alpha=0} y_\alpha^k H(y_\alpha) \tag{14}$$

$$Q_r = KhG_{rz} \sum_{\alpha=1}^{2} \sum_{k=0}^{4} \frac{1}{k!} \left(-X_{(k)}^{(\alpha)} G^{(\alpha)^{-1}} + \frac{\delta X_{(k-1)}^{(\alpha)}}{\delta t} G^{(\alpha)^{-1}} - \omega_{(k-1)}^{(\alpha)} \right)\Bigg|_{y_\alpha=0} y_\alpha^k H(y_\alpha) \tag{15}$$

where $y_\alpha = t - (r - r_0)G^{(\alpha)^{-1}}$.

4. Determination of arbitrary constants and solution analysis at $N < N^{\mathrm{crit}}$

Relationships Eqs (14) and (15) involve two sets of unknown constants $c_i^{(1)}$ and $c_i^{(2)}$ $(i = 0, 1, 2, 3),$ which are determined from three dynamic conditions of contact (2)–(4). In order the number of arbitrary constants to be in compliance with the number of contact conditions, it is a need to introduce one more set of unknown constants by representing the function $\alpha(t)$ in the form

$$\alpha(t) = \sum_{i=0}^{6} \alpha_i t^i \tag{16}$$

where α_i $(i = 0, 1, 2, \ldots 6)$.

Substituting Eqs (14)–(16) with due account for Eqs (12) and (13) in Eqs (2)–(4), having regard to expression Eq. (1) and the initial conditions Eq. (5), and equating the coefficients at like powers of t in the relationships obtained, we find at each step three algebraic equations for determining the three unknown constants: two of them at each t enter into the ray series for W and Q_r, and one constant at each t is held in Eq. (16). Thus, we have

$$c_0^{(1)} = c_0^{(2)} = c_1^{(2)} = \alpha_0 = \alpha_2 = 0, \quad \alpha_1 = V_0$$

$$\alpha_3 = -\frac{E_1 V_0}{6} \left(\frac{1}{m} + \frac{1}{\rho h \pi r_0^2} \right), \quad \alpha_4 = \frac{E_1 V_0 (G^{(1)} + G^{(2)})}{12 \rho h \pi r_0^3}$$

$$c_1^{(1)} = \frac{a E_1 V_0 (G^{(1)} + G^{(2)})}{\rho h \pi r_0^{3/2} G^{(2)^2}}, \quad c_2^{(2)} = -\frac{E_1 V_0 G^{(2)}}{\rho h \pi r_0^{3/2} (G^{(1)} - G^{(2)})}$$

$$c_2^{(1)} = -\frac{a E_1 V_0 G^{(1)} (G^{(1)} + G^{(2)})}{2 \rho h \pi r_0^{5/2} G^{(2)^2}} \left[\frac{b_r}{a} \left(1 - a - \frac{1}{e_r} \right) r_0^2 + \left(\frac{E_\theta}{E_r} - 1 \right) + \frac{15}{4} + 3 \frac{G^{(2)}}{G^{(1)}} \right]$$

$$c_3^{(2)} = \frac{E_1 V_0 G^{(2)^2}}{2 \rho h \pi r_0^{5/2} (G^{(1)} - G^{(2)})} \left(\frac{b_r r_0^2}{a e_r} + \frac{15}{4} + 3 \frac{G^{(1)}}{G^{(2)}} \right) \tag{17}$$

$$\alpha_5 = -\frac{E_1 V_0 (G^{(1)} + G^{(2)})^2}{40 \rho h \pi r_0^4} + \frac{E_1^2 V_0}{120} \left(\frac{1}{m} + \frac{2}{\rho h \pi r_0^2} \right) \left(\frac{1}{m} + \frac{1}{\rho h \pi r_0^2} \right)$$

$$\alpha_6 = \frac{E_1V_0(G^{(1)}+G^{(2)})^3}{180\rho h\pi r_0^5} - \frac{E_1V_0({G^{(1)}}^3+{G^{(2)}}^3)}{2880\rho h\pi r_0^5} - \frac{E_1^2V_0(G^{(1)}+G^{(2)})}{360\rho h\pi r_0^3}\left(\frac{3}{m}+\frac{4}{\rho h\pi r_0^2}\right)$$
$$- \frac{E_1V_0{G^{(2)}}^2({G^{(1)}}^3-{G^{(2)}}^3)}{60a^2\rho h^3\pi r_0^3({G^{(1)}}^2-{G^{(2)}}^2)} + \frac{E_1V_0{G^{(1)}}^3G^{(2)}}{720\rho h\pi r_0^5(G^{(1)}-G^{(2)})}\left(\frac{E_\theta}{E_r}-1\right) - \frac{E_1V_0(a-1)G^{(1)}{G^{(2)}}^2}{60a^2\rho h^3\pi r_0^3}$$

$$c_3^{(1)} = \frac{aE_1V_0(G^{(1)}+G^{(2)})}{\rho h\pi r_0^{3/2}{G^{(2)}}^2}\left[\frac{{G^{(1)}}^2b_r^2r_0^2}{8a^2}\left(1-a-\frac{1}{e_r}\right)^2 + \frac{{G^{(1)}}^2}{8r_0^2}\left(\frac{E_\theta}{E_r}-1\right)^2 - \frac{39{G^{(1)}}^2}{128r_0^2}\right.$$
$$+\frac{{G^{(1)}}^2b_r}{2a}\left(1-a-\frac{1}{e_r}\right)\left(\frac{E_\theta}{E_r}-1\right) + \frac{3G^{(1)}(G^{(1)}-G^{(2)})}{4r_0^2}\left(\frac{E_\theta}{E_r}-1\right) + \frac{13{G^{(1)}}^2b_r}{8a}\left(1-a-\frac{1}{e_r}\right)$$
$$+\frac{{G^{(1)}}^2}{f_rr_0^2}\left(\frac{E_\theta}{E_r}-1\right) - \frac{{G^{(1)}}^2b_r}{af_r}\left(1-a-\frac{1}{e_r}\right) + \frac{3G^{(1)}G^{(2)}b_r}{4a}\left(1-a-\frac{1}{e_r}\right)$$
$$+\frac{3(G^{(1)}+G^{(2)})^2}{r_0^2} - \frac{3G^{(1)}G^{(2)}}{16r_0^2} - E_1\left(\frac{1}{m}+\frac{2}{\rho h\pi r_0^2}\right) - \frac{9G^{(2)}(G^{(1)}+G^{(2)})}{8r_0^2}$$
$$\left.+\frac{{G^{(1)}}^2G^{(2)}}{2r_0^2(G^{(1)}-G^{(2)})}\left(\frac{E_\theta}{E_r}-1\right) + \frac{{G^{(1)}}^2G^{(2)}}{2a(G^{(1)}-G^{(2)})}\left(a-1+\frac{{G^{(1)}}^2+{G^{(2)}}^2}{{G^{(1)}}^2-{G^{(2)}}^2}\right)\right]$$

$$c_4^{(2)} = \frac{E_1V_0G^{(2)}}{\rho h\pi r_0^{3/2}(G^{(1)}-G^{(2)})}\left[E_1\left(\frac{1}{m}+\frac{2}{\rho h\pi r_0^2}\right) - \frac{3(G^{(1)}+G^{(2)})^2}{r_0^2} + \frac{9G^{(1)}(G^{(1)}+G^{(2)})}{8r_0^2}\right.$$
$$- \frac{{G^{(1)}}^3}{2r_0^2(G^{(1)}-G^{(2)})}\left(\frac{E_\theta}{E_r}-1\right) - \frac{{G^{(2)}}^2G^{(1)}b_r}{2ae_r(G^{(1)}-G^{(2)})} - \frac{{G^{(1)}}^3b_r(a-1)}{2ae_r(G^{(1)}-G^{(2)})} + \frac{9{G^{(2)}}^2}{128r_0^2}$$
$$\left.+\frac{b_r^2r_0^2}{8a^2e_r^2} + \frac{{G^{(2)}}^2}{4}\left(\frac{b_rr_0^2}{ae_r}+\frac{15}{4}+\frac{3G^{(1)}}{G^{(2)}}\right)\left(\frac{1}{4r_0^2}-\frac{b_r}{ae_r}\right)\right]$$

Knowing the constants Eq. (17), one could determine the contact force and the displacement of the contact spot with the accuracy of t^6 in the following form:

$$\frac{P(t)}{E_1} = V_0t - \frac{E_1V_0}{6}\left(\frac{1}{m}+\frac{2}{M}\right)t^3 + \frac{E_1V_0(G^{(1)}+G^{(2)})}{6Mr_0}\,t^4$$
$$- \frac{E_1V_0}{20M}\left[\frac{(G^{(1)}+G^{(2)})^2}{r_0^2} - \frac{E_1}{6}\left(\frac{1}{m}+\frac{2}{M}\right)^2\right]t^5 + \frac{E_1V_0}{90Mr_0}\left[\frac{(G^{(1)}+G^{(2)})^3}{r_0^2}\right.$$
$$- \frac{{G^{(1)}}^3+{G^{(2)}}^3}{16r_0^2} - E_1(G^{(1)}+G^{(2)})\left(\frac{1}{m}+\frac{2}{M}\right) - \frac{3{G^{(2)}}^2({G^{(1)}}^3-{G^{(2)}}^3)}{a^2h^2({G^{(1)}}^2-{G^{(2)}}^2)}$$
$$\left.+\frac{{G^{(1)}}^3G^{(2)}}{4r_0^2(G^{(1)}-G^{(2)})}\left(\frac{E_\theta}{E_r}-1\right) + \frac{3(1-a){G^{(2)}}^2G^{(1)}}{a^2h^2}\right]t^6 \tag{18}$$

$$w(t) = \frac{E_1V_0}{M}\,\frac{t^3}{6} - \frac{E_1V_0(G^{(1)}+G^{(2)})}{Mr_0}\,\frac{t^4}{12} + \left[\frac{3E_1V_0(G^{(1)}+G^{(2)})^2}{Mr_0^2}\right.$$
$$\left.- \frac{E_1^2V_0}{M}\left(\frac{1}{m}+\frac{2}{M}\right)\right]\frac{t^5}{120} + \left[\frac{2E_1^2V_0(G^{(1)}+G^{(2)})}{Mr_0}\left(\frac{1}{m}+\frac{4}{M}\right)\right.$$
$$\left.- \frac{4E_1V_0(G^{(1)}+G^{(2)})^3}{Mr_0^3} + \frac{E_1V_0({G^{(1)}}^3+{G^{(2)}}^3)}{4Mr_0^3} + \frac{12E_1V_0{G^{(2)}}^2({G^{(1)}}^3-{G^{(2)}}^3)}{Mr_0a^2h^2({G^{(1)}}^2-{G^{(2)}}^2)}\right. \tag{19}$$

$$- \frac{E_1 V_0 {G^{(1)}}^3 G^{(2)}}{M r_0^3 (G^{(1)} - G^{(2)})} \left(\frac{E_\theta}{E_r} - 1 \right) + \frac{12 E_1 V_0 (a-1) {G^{(2)}}^2 G^{(1)}}{M r_0 a^2 h^2} \Bigg] \frac{t^6}{720}$$

Since the duration of the shock interaction process is short, then the approximation of the desired functions within the contact domain by the truncated power series with respect to time with an accuracy of t^6 is reasonably fair one.

Reference to the expressions Eqs (18) and (19) shows that the parameter a varies from the unit ($N = 0$) to zero ($N = N^{\rm crit} = hKG_{rz}$). Thus, these simple analytical relationships for the contact force Eq. (18) and the plate's deflection Eq. (19) for any compressive force less than the critical one may be easily implemented in engineering practice required the analysis of low-velocity behavior of precompressed orthotropic plates.

The most interesting is the case of $N = N^{\rm crit}$ $(a = 0, G^{(2)} = 0)$, since in this case the plate occurs in the critical state. All terms entering into the values $w(r,t)$ and $Q_r(r,t)$ and involving the parameter a and the velocity $G^{(2)}$ possess the uncertainty of $0/0$ type when $a \to 0$, which can be removed due to L'Hospital rule.

5. Analysis of the system's critical state

Let the compression force N in the orthotropic plate attain its critical magnitude. Then as a result of impact of a body upon the elastic orthotropic plate, only one wave is generated in the plate which further propagates with the velocity $G^{(1)}$, but the second wave turns out to be 'locked' within the contact region. In this case, the main characteristics of shock interaction have the form

$$\begin{aligned}
&\frac{M}{E_1 V_0} \left(\frac{r}{r_0} \right)^{1/2} w^{\rm crit}(r,t) = \frac{1}{6}\, y_1^3 - \frac{1}{48}\, G^{(1)} \left[\left(\frac{E_\theta}{E_r} - 1 \right) \frac{(r - r_0)}{r_0 r} + b_r (r - r_0) + \frac{4}{r_0} \right] y_1^4 \\
&+ \frac{1}{120}\, {G^{(1)}}^2 \left\{ \frac{1}{4 r_0} \left[\left(\frac{E_\theta}{E_r} - \frac{5}{4} \right) - b_r r_0^2 + 4 \right] \left[\left(\frac{E_\theta}{E_r} - \frac{5}{4} \right) \frac{(r - r_0)}{r_0 r} + b_r (r - r_0) \right] \right. \\
&\left. + \frac{1}{8} \left[- \left(\frac{E_\theta}{E_r} - \frac{1}{4} \right)^2 \frac{(r^2 - r_0^2)}{r_0^2 r^2} + b_r^2 (r - r_0)^2 \right] + \frac{3}{r_0^2} - \frac{E_1}{{G^{(1)}}^2} \left(\frac{1}{m} + \frac{2}{M} \right) \right\} y_1^5
\end{aligned} \tag{20}$$

$$\begin{aligned}
&- \frac{\pi r_0^2}{E_1 V_0 G^{(1)}} \left(\frac{r}{r_0} \right)^{1/2} Q_r^{\rm crit}(r,t) = \frac{1}{2}\, y_1^2 - \frac{1}{12}\, \frac{G^{(1)}}{r} \left[\left(\frac{E_\theta}{E_r} - \frac{1}{4} \right) \left(\frac{r}{r_0} - 1 \right) + b_r r (r - r_0) + \frac{3r}{r_0} \right] y_1^3 \\
&+ \frac{1}{24}\, \frac{{G^{(1)}}^2}{r^2} \left\{ \frac{1}{4} \left(\frac{E_\theta}{E_r} - \frac{1}{4} + 3 - b_r r_0^2 \right) \left[\left(\frac{E_\theta}{E_r} - \frac{1}{4} \right) \left(\frac{r}{r_0} - 1 \right) - \frac{r}{r_0} + b_r r (r - r_0) \right] \frac{r}{r_0} \right. \\
&+ 3\, \frac{r^2}{r_0^2} - \frac{3}{4}\, b_r r^2 - \frac{1}{8} \left[\left(\frac{E_\theta}{E_r} - \frac{1}{4} \right)^2 \left(\frac{r^2}{r_0^2} - 1 \right) - b_r^2 r^2 (r^2 - r_0^2) \right] - \frac{E_1}{{G^{(1)}}^2} \left(\frac{1}{m} + \frac{2}{M} \right) r^2 \\
&\left. + \frac{K G_{rz}}{B_r} \left(\frac{E_\theta}{E_r} - 1 + b_r r^2 \right) \right\} y_1^4
\end{aligned} \tag{21}$$

Putting $r = r_0$ in Eqs (20) and (21) yields

$$\begin{aligned}
w^{\rm crit}(t) = \frac{E_1 V_0}{M} \left\{ \frac{t^3}{6} - \frac{G^{(1)} t^4}{12 r_0} + \left[\frac{3 {G^{(1)}}^2}{r_0^2} - E_1 \left(\frac{1}{m} + \frac{2}{M} \right) \right] \frac{t^5}{120} \right. \\
\left. - \left[\frac{15 {G^{(1)}}^3}{4 r_0^3} - \frac{2 E_1 G^{(1)}}{r_0} \left(\frac{1}{m} + \frac{4}{M} \right) \right] \frac{t^6}{720} \right\}
\end{aligned} \tag{22}$$

$$\begin{aligned}
Q_r^{\rm crit}(t) = - \frac{E_1 V_0 G^{(1)}}{\pi r_0^2} \left\{ \frac{t^2}{2} - \frac{G^{(1)} t^3}{4 r_0} + \frac{{G^{(1)}}^2}{r_0^2} \left[\frac{K G_{rz}}{B_r} \left(\frac{E_\theta}{E_r} - 1 + b_r r^2 \right) \right. \right. \\
\left. \left. - \frac{E_1 r_0^2}{{G^{(1)}}^2} \left(\frac{1}{m} + \frac{2}{M} \right) + 3 - \frac{3}{4}\, b_r r_0^2 - \frac{1}{4} \left(\frac{E_\theta}{E_r} - 1 + \frac{15}{4} - b_r r_0^2 \right) \right] \frac{t^4}{24} \right\}
\end{aligned} \tag{23}$$

Along with Eqs (22) and (23) the expression for the contact force could be written

$$P^{\rm crit}(t)=E_1V_0\left\{t-E_1\left(\frac{1}{m}+\frac{2}{M}\right)\frac{t^3}{6}+\frac{E_1G^{(1)}}{Mr_0}\,\frac{t^4}{6}-\,\frac{E_1}{M}\left[\frac{{G^{(1)}}^2}{r_0^2}-\frac{E_1}{6}\left(\frac{1}{m}+\frac{2}{M}\right)^2\right]\frac{t^5}{20}\right.$$
$$\left.+\frac{E_1G^{(1)}}{Mr_0}\left[\frac{{G^{(1)}}^2}{16r_0^2}-\frac{E_1}{15}\left(\frac{1}{m}+\frac{2}{M}\right)\right]\frac{t^6}{6}\right\} \tag{24}$$

Equations (22)–(24) are quite important for designers of composite structures, since they can provide a basic understanding of the structural response in the critical state and how it is affected by different parameters, giving a foundation for prediction of impact damage.

6. Numerical example

To analyze the results obtained, let us consider a numerical example. For this purpose, rewrite expressions Eqs (18)–(24) in the dimensionless form

$$\widetilde{w}(\widetilde{t})=\frac{\widetilde{E}\widetilde{V}}{\pi\widetilde{h}}\left\{\frac{\widetilde{t}^3}{6}-\left(1+\frac{G^{(2)}}{G^{(1)}}\right)\frac{\widetilde{t}^4}{12}+\left[\left(1+\frac{G^{(2)}}{G^{(1)}}\right)^2-\,\frac{\widetilde{E}}{3\pi\widetilde{h}}(\widetilde{m}+2)\right]\frac{\widetilde{t}^5}{40}\right.$$
$$+\left[\frac{\widetilde{E}}{6\pi\widetilde{h}}\left(1+\frac{G^{(2)}}{G^{(1)}}\right)(\widetilde{m}+4)-\,\frac{1}{3}\left(1+\frac{G^{(2)}}{G^{(1)}}\right)^3+\frac{1}{48}\left(1+\frac{{G^{(2)}}^3}{{G^{(1)}}^3}\right)\right.$$
$$+\frac{1}{a^2\widetilde{h}^2}\,\frac{{G^{(2)}}^2}{{G^{(1)}}^2}\left(1-\frac{{G^{(2)}}^3}{{G^{(1)}}^3}\right)\left(1-\frac{{G^{(2)}}^2}{{G^{(1)}}^2}\right)^{-1}-\,\frac{1-a}{a^2\widetilde{h}^2}\,\frac{{G^{(2)}}^2}{{G^{(1)}}^2}$$
$$\left.\left.-\,\frac{1}{12}\left(\frac{E_\theta}{E_r}-1\right)\left(1-\frac{G^{(2)}}{G^{(1)}}\right)^{-1}\frac{G^{(2)}}{G^{(1)}}\right]\frac{\widetilde{t}^6}{60}\right\} \tag{25}$$

$$\widetilde{P}(\widetilde{t})=\widetilde{V}\left\{\widetilde{t}-\,\frac{\widetilde{E}}{\pi\widetilde{h}}(\widetilde{m}+2)\frac{\widetilde{t}^3}{6}+\frac{\widetilde{E}}{\pi\widetilde{h}}\left(1+\frac{G^{(2)}}{G^{(1)}}\right)\frac{\widetilde{t}^4}{6}-\,\frac{\widetilde{E}}{\pi\widetilde{h}}\left[\left(1+\frac{G^{(2)}}{G^{(1)}}\right)^2\right.\right.$$
$$\left.-\,\frac{\widetilde{E}}{6\pi\widetilde{h}}(\widetilde{m}+2)^2\right]\frac{\widetilde{t}^5}{20}+\,\frac{\widetilde{E}}{\pi\widetilde{h}}\left[\left(1+\frac{G^{(2)}}{G^{(1)}}\right)^3-\,\frac{\widetilde{E}}{\pi\widetilde{h}}\left(1+\frac{G^{(2)}}{G^{(1)}}\right)(\widetilde{m}+2)\right.$$
$$-\,\frac{1}{16}\left(1+\frac{{G^{(2)}}^3}{{G^{(1)}}^3}\right)-\,\frac{3}{a^2\widetilde{h}^2}\,\frac{{G^{(2)}}^2}{{G^{(1)}}^2}\left(1-\frac{{G^{(2)}}^3}{{G^{(1)}}^3}\right)\left(1-\frac{{G^{(2)}}^2}{{G^{(1)}}^2}\right)^{-1}$$
$$\left.\left.+\frac{3(1-a)}{a^2\widetilde{h}^2}\,\frac{{G^{(2)}}^2}{{G^{(1)}}^2}+\frac{1}{4}\left(\frac{E_\theta}{E_r}-1\right)\left(1-\frac{G^{(2)}}{G^{(1)}}\right)^{-1}\frac{G^{(2)}}{G^{(1)}}\right]\frac{\widetilde{t}^6}{90}\right\} \tag{26}$$

$$\widetilde{w}^{\rm crit}(\widetilde{t})=\frac{\widetilde{E}\widetilde{V}}{\pi\widetilde{h}}\left\{\frac{\widetilde{t}^3}{6}-\,\frac{\widetilde{t}^4}{12}+\left[1-\,\frac{\widetilde{E}}{3\pi\widetilde{h}}(\widetilde{m}+2)\right]\frac{\widetilde{t}^5}{40}+\left[\frac{2\widetilde{E}}{\pi\widetilde{h}}(\widetilde{m}+4)-\,\frac{15}{4}\right]\frac{\widetilde{t}^6}{720}\right\} \tag{27}$$

$$\widetilde{P}^{\rm crit}(\widetilde{t})=\widetilde{V}\left\{\widetilde{t}-\,\frac{\widetilde{E}}{\pi\widetilde{h}}(\widetilde{m}+2)\frac{\widetilde{t}^3}{6}+\frac{\widetilde{E}}{\pi\widetilde{h}}\frac{\widetilde{t}^4}{6}-\,\frac{\widetilde{E}}{\pi\widetilde{h}}\left[1-\,\frac{\widetilde{E}}{6\pi\widetilde{h}}(\widetilde{m}+2)^2\right]\frac{\widetilde{t}^5}{20}\right.$$
$$\left.+\,\frac{\widetilde{E}}{\pi\widetilde{h}}\left[\frac{1}{16}-\,\frac{\widetilde{E}}{15\pi\widetilde{h}}(\widetilde{m}+2)\right]\frac{\widetilde{t}^6}{6}\right\} \tag{28}$$

$$\widetilde{Q}_r^{\rm crit}(\widetilde{t}) = -\widetilde{V}\left\{\frac{\widetilde{t}^2}{2} - \frac{\widetilde{t}^3}{4} + \left[\frac{KG_{rz}}{B_r}\left(\frac{E_\theta}{E_r} - 1 + \frac{12}{\widetilde{h}^2}\,\frac{KG_{rz}}{B_r}\right) - \frac{\widetilde{E}}{\pi\widetilde{h}}(\widetilde{m}+2) + 3 \right.\right.$$
$$\left.\left. - \frac{9}{\widetilde{h}^2}\,\frac{KG_{rz}}{B_r} - \frac{1}{4}\left(\frac{E_\theta}{E_r} - 1 + \frac{15}{4} - \frac{12}{\widetilde{h}^2}\,\frac{KG_{rz}}{B_r}\right)\right]\frac{\widetilde{t}^4}{24}\right\} \tag{29}$$

$$\widetilde{Q}_r^{\rm crit}(\widetilde{r},\widetilde{t})\widetilde{V}^{-1} = -\frac{1}{2}\,\widetilde{r}^{-1/2}\left(\widetilde{t}+1-\widetilde{r}\right)^2 + \frac{1}{12}\,\widetilde{r}^{-3/2}\left[\left(\frac{E_\theta}{E_r} - \frac{1}{4}\right)(\widetilde{r}-1)\right.$$
$$\left. + \frac{12}{\widetilde{h}^2}\,\frac{KG_{rz}}{B_r}\widetilde{r}(\widetilde{r}-1) + 3\widetilde{r}\right]\left(\widetilde{t}+1-\widetilde{r}\right)^3 - \frac{1}{24}\,\widetilde{r}^{-5/2}\left\{\frac{1}{4}\left(\frac{E_\theta}{E_r} - \frac{1}{4} + 3\right.\right.$$
$$\left. - \frac{12}{\widetilde{h}^2}\,\frac{KG_{rz}}{B_r}\right)\left[\left(\frac{E_\theta}{E_r} - \frac{1}{4}\right)(\widetilde{r}-1) - \widetilde{r} + \frac{12}{\widetilde{h}^2}\,\widetilde{r}(\widetilde{r}-1)\right]\widetilde{r} + 3\widetilde{r}^2 \tag{30}$$
$$- \frac{9}{\widetilde{h}^2}\,\frac{KG_{rz}}{B_r}\widetilde{r}^2 - \frac{1}{8}\left[\left(\frac{E_\theta}{E_r} - \frac{1}{4}\right)^2(\widetilde{r}^2-1) - \left(\frac{12}{\widetilde{h}^2}\,\frac{KG_{rz}}{B_r}\right)^2\widetilde{r}^2(\widetilde{r}^2-1)\right]$$
$$\left. - \frac{\widetilde{E}}{\pi\widetilde{h}}(\widetilde{m}+2)\widetilde{r}^2 + \frac{KG_{rz}}{B_r}\left(\frac{E_\theta}{E_r} - 1 + \frac{12}{\widetilde{h}^2}\,\frac{KG_{rz}}{B_r}\,\widetilde{r}^2\right)\right\}\left(\widetilde{t}+1-\widetilde{r}\right)^4$$

$$\widetilde{w}^{\rm crit}(\widetilde{r},\widetilde{t})\frac{\pi\widetilde{h}}{\widetilde{E}\widetilde{V}} = \frac{1}{6}\,\widetilde{r}^{-1/2}\left(\widetilde{t}+1-\widetilde{r}\right)^3 - \frac{1}{48}\,\widetilde{r}^{-3/2}\left[\left(\frac{E_\theta}{E_r} - 1\right)(\widetilde{r}-1)\right. \tag{31}$$
$$\left. + \frac{12}{\widetilde{h}^2}\,\frac{KG_{rz}}{B_r}(\widetilde{r}-1) + 4\widetilde{r}\right]\left(\widetilde{t}+1-\widetilde{r}\right)^4$$
$$+ \frac{1}{120}\left\{\frac{1}{4}\,\widetilde{r}^{-3/2}\left[\left(\frac{E_\theta}{E_r} - \frac{5}{4}\right) - \frac{12}{\widetilde{h}^2}\,\frac{KG_{rz}}{B_r} + 4\right]\left[\left(\frac{E_\theta}{E_r} - \frac{5}{4}\right) + \frac{12}{\widetilde{h}^2}\,\frac{KG_{rz}}{B_r}\right](\widetilde{r}-1)\right.$$
$$\left. + \frac{1}{8}\,\widetilde{r}^{-5/2}\left[\frac{12}{\widetilde{h}^2}\,\frac{KG_{rz}}{B_r} - \left(\frac{E_\theta}{E_r} - \frac{1}{4}\right)^2\right](\widetilde{r}^2-1) + 3\widetilde{r}^{-3/2} - \frac{\widetilde{E}}{\pi\widetilde{h}}(\widetilde{m}+2)\right\}\left(\widetilde{t}+1-\widetilde{r}\right)^5$$

where $\widetilde{w} = wr_0^{-1}$, $\widetilde{P} = P(E_1 r_0)^{-1}$, $\widetilde{Q}_r = Q_r(\pi E_1)^{-1}$, $\widetilde{t} = G^{(1)}r_0^{-1}t$, $\widetilde{r} = rr_0^{-1}$, $\widetilde{V} = V_0 {G^{(1)}}^{-1}$, $\widetilde{E} = E_1(r_0 B_r)^{-1}$, $\widetilde{h} = hr_0^{-1}$, and $\widetilde{m} = Mm^{-1}$.

The curves for the $\widetilde{t}$-dependence of $\widetilde{w}$ and $\widetilde{P}$ are presented in Figs 2 through 4 for three magnitudes of the ratio E_θ/E_r: 2 (Fig. 2), 1 (Fig. 3), and 2/3 (Fig. 4). The curves in Figs 2 through 4 correspond to the following magnitudes of the value a: 1, 0.75, 0.5, 0.25, and 0. At $a = 1$, the initial compression is absent, but at $a = 0$ the magnitude of the compression force attains its critical magnitude, at which the maximal magnitudes of the values $\widetilde{w}$ and $\widetilde{P}$ possess the largest magnitudes among all maximal magnitudes of the given values, corresponding to the parameter $0 < a \leqslant 1$. The contact time is also reaches its maximum at $a = 0$. Thus, reference to Figs 2 through 4 shows that the curves at $a = 0$ are the limiting ones for all other curves corresponding to the parameter $0 < a \leqslant 1$.

Figures 2 through 4 also indicate that the decrease in the ratio E_θ/E_r elevates the maximum contact force and the contact time, but reduces the peak deflection.

When $a < 0$, the critical state of the plate is changed by its post-critical state. In this case, square of the velocity $G^{(2)}$ takes on a negative value, and the governing set of equations of a hyperbolic type goes over into an elliptic one. That is why, at $a < 0$ the solution obtained is not applicable. But even without detail analysis of the case $a < 0$, the following considerations could be made about the post-critical behavior of the plate: since all energy of shock interaction is concentrated in the contact region (the wave is 'locked' within this domain), then this may result in damage of the structure within the contact zone. It seems likely that at the post-critical state, the rigid washer (the contact region) is cut off with its further knocking out of the plate.

In order to illustrate this conclusion, let us consider an idealized system.

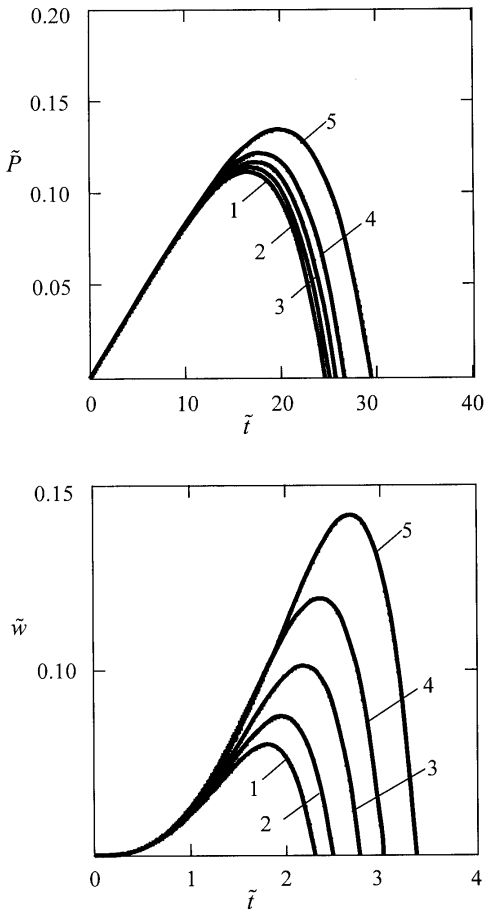

Fig. 2. The dimensionless time dependence of the dimensionless contact force and deflection at $E_\theta/E_r = 2$ for $a = 1$ (curve 1), 0.75 (curve 2), 0.5 (curve 3), 0.25 (curve 4), and 0 (curve 5).

7. An idealized system and its analysis

To visualize pictorially how the character of the system behavior changes during transition from an ordinary state to the critical one, let us consider an idealized system consisting of a thin elastic infinite plate which responses only to shear deformations. The equation of motion of such a plate is obtained from Eq. (7) if one neglects the terms involving the value φ. As a result we have

$$\ddot{w} - G_0^{(2)^2} a\Delta w = 0 \tag{32}$$

where $G_0^{(2)^2} = KG_{rz}\rho^{-1}$.

Shock excitation of the given plate is changed for the instantaneous application of constant velocity to a certain region $0 \leqslant r \leqslant r_0$ at the initial instant of time, i.e.,

$$w\Big|_{t=0} = 0, \quad \dot{w}\Big|_{t=0} = V_0 H(r_0 - r) \tag{33}$$

Applying the zeroth order Hankel transformation to Eqs (32) and (33) and considering that

$$\overline{\Delta w} = \int_0^\infty r\Delta w J_0(kr)dr = \int_0^\infty r\left(\frac{\partial^2 w}{\partial r^2} + \frac{1}{r}\,\frac{\partial w}{\partial r}\right) J_0(kr)dr = -k^2\overline{w}(k,t)$$

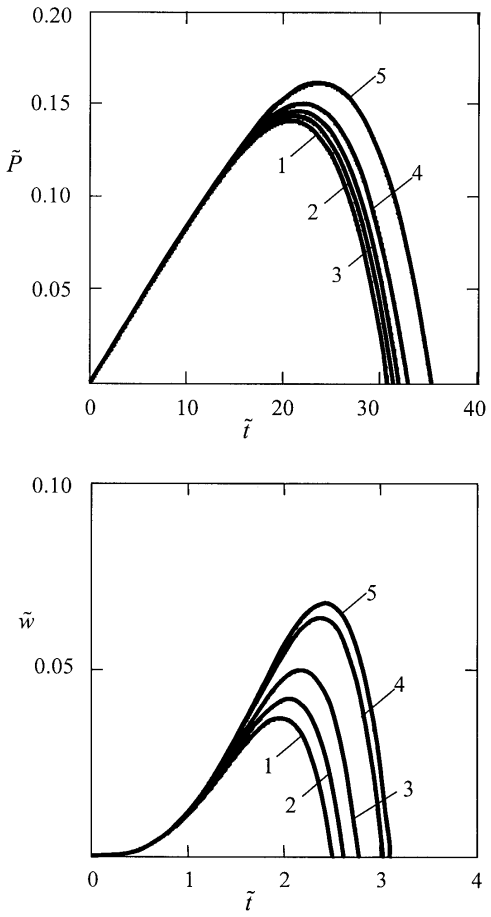

Fig. 3. The dimensionless time dependence of the dimensionless contact force and deflection at $E_\theta/E_r = 1$ for $a = 1$ (curve 1), 0.75 (curve 2), 0.5 (curve 3), 0.25 (curve 4), and 0 (curve 5).

$$\overline{H}(r_0 - r) = r_0 k^{-1} J_1(kr_0) \tag{34}$$

where a bar over the values denotes zeroth order Hankel transform, k is the variable of this transformation, we have

$$\ddot{\overline{w}} + k^2 {G_0^{(2)}}^2 a\, \overline{w} = 0 \tag{35}$$

$$\overline{w}(k, 0) = 0 \tag{36}$$

$$\dot{\overline{w}}(k, 0) = V_0 r_0 k^{-1} J_1(kr_0) \tag{37}$$

When $a > 0$, solution of Eq. (35) subjected to the condition Eq. (36) has the form

$$\overline{w}(k, t) = C(k) \sin\left(kG_0^{(2)}\sqrt{a}\, t\right) \tag{38}$$

where $C(k)$ is an arbitrary function.

To find the function $C(k)$, differentiate expression Eq. (38) with respect to t. Then we obtain

$$\dot{\overline{w}}(k, t) = C(k) k G_0^{(2)} \sqrt{a} \cos\left(kG_0^{(2)}\sqrt{a}\, t\right) \tag{39}$$

Putting $t = 0$ in Eq. (39) and taking the initial condition Eq. (37) into account yields

$$C(k) = \frac{V_0 r_0}{G_0^{(2)}\sqrt{a}\, k^2}\, J_1(kr_0) \tag{40}$$

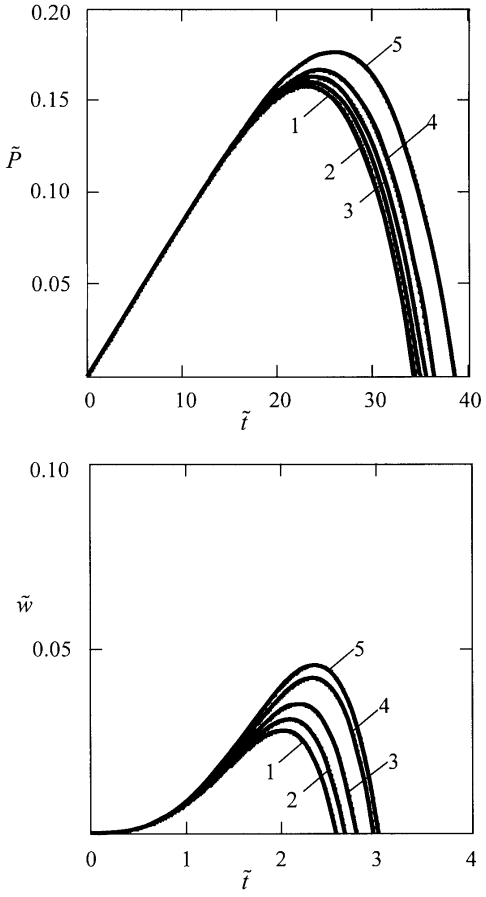

Fig. 4. The dimensionless time dependence of the dimensionless contact force and deflection at $E_\theta/E_r = 2/3$ for $a = 1$ (curve 1), 0.75 (curve 2), 0.5 (curve 3), 0.25 (curve 4), and 0 (curve 5).

Considering (40), the expression for $w(r,t)$ takes the form

$$w = \begin{cases} \frac{V_0 r_0}{G_0^{(2)}\sqrt{a}} \int\limits_0^\infty k^{-1} J_1(kr_0) J_0(kr) \sin\left(kG_0^{(2)}\sqrt{a}\, t\right) dk, & \left(r - r_0 < G_0^{(2)}\sqrt{a}\, t\right) \\ 0, & \left(r - r_0 > G_0^{(2)}\sqrt{a}\, t\right) \end{cases} \tag{41}$$

Tending the value a to zero in (41) yields

$$w = \begin{cases} V_0 r_0 t \int\limits_0^\infty J_1(kr_0) J_0(kr) dk = V_0 t, & (r < r_0) \\ 0, & (r > r_0) \end{cases} \tag{42}$$

From Eqs (41) and (42) it follows that before the critical state the plate deflection at $r_0 \le r < G_0^{(2)}\sqrt{a}\, t$ varies with time by the harmonic law, and it is nonzero within the whole domain of transverse shear wave propagation. In the critical state, the wave is completely 'locked' within the region of action of the constant velocity of displacement, where the deflection $w = V_0 t$, but in the rest region $w = 0$. If $a < 0$, what corresponds to the post-critical state of the plate, then in the expression for w an ordinary sine is substituted by a hyperbolic one, and the given expression loses its meaning.

Based on the examples considered, the following conclusion could be drawn: a circular orthotropic plate uniformly compressed by the radial forces $N = N^{\rm crit} = hKG_{rz}$ is under the critical state with respect to impact excitation, i.e. at $N > N^{\rm crit}$ any as small as is wished subjection of velocity to the rigid washer (the contact zone) results in its cut off with further knocking out of the plate.

8. Discussion

Investigators, who studied impact response of prestressed composite plates [6,13], made one and the same conclusion: the tensile initial stresses induce a stiffening effect on the plate, since the peak deflection of the plate at the contact region is less than the maximal deflection of the plate under the initial compressive stresses at the same place, and hence the initial compressive stress appears to cause a softening effect on the plate stiffness. But this is not quite the case. As the analysis carried out in the present paper shows, the velocity of the transient wave of transverse shear begins to decrease with the increase in the compression force, resulting in reducing magnitudes of the stress discontinuities on this wave. When reaching the critical magnitude of the compression force, the transverse shear wave is 'locked' at all in the contact domain. The occurrence of such an effect may be attributable to the fact that under intense compression of the plate material in the critical state, atoms are brought closer together, and atomic lattice is compressed. There is no way of shearing the atoms in such a lattice, therefore the transient shear wave attenuates quickly lossing all its energy at the moment of its generation. Similar effect is observed in a highly compressed gas during the propagation of short compression waves through the gas, which is known as Landau attenuation. Thus, since all shear energy of the impactor is concentrated in the contact domain, then this may result in plate damage within this region, and hence in the increase of the peak deflection at this place.

As for the impact response of the pretensioned plate, then an opposite situation takes place, namely: a higher initial tensile force elevates the velocity of the transient wave of transverse shear, resulting in an increase in magnitudes of the stress discontinuities on this wave. Therefore, the bulk energy of shock interaction is imparted to the transient wave of transverse shear, and the lesser part of energy is passed on the contact zone. Because of this, damage within the contact region and the magnitude of the maximal deflection in the case of the pretensioned plate are less than those of the precompressed plate. This conclusion is supported by experiments [13].

9. Conclusions

The low-velocity impact response of a precompressed circular orthotropic plate is investigated, which is important in damage-tolerant design of composite material structures. Contact interaction between the impactor and the target is modeled by a linear spring, and a force arising in it is the linear approximation of Herts'z contact force. The dynamic behavior of the plate is described by equations taking the rotary inertia and transverse shear deformations into account. Longitudinal compressing forces are uniformly distributed along the plate's median plane. Stability or instability of the plate is established by analyzing the behavior of transient waves generating in the plate at the moment of impact, which further propagate along its median surface as 'diverging circles'.

From the trends of the results of the present day, the following conclusions may be drawn:

1. The present work gives an analytical solution to the problem of low-velocity impact on a circular precompressed plate, based on the ray method. Simple analytical relationships for the contact force and plate's deflection are obtained for any compressive force less than the critical one, which are applicable for engineering calculations required the analysis of impact response of preloaded structures.
2. The critical magnitude of the compression force is found, at which 'locking' of the transient wave of transverse shear occurs within the contact region. This leads to the fact that all shear energy during impact is concentrated within the contact zone. The analytical solution describing the interaction of the impactor with the plate in the critical state is obtained. As far as the authors know, such a phenomenon in a precompressed elastic plate has not been described in scientific literature to the present day.
3. It is shown that under the compression force larger than the critical one, the hyperbolic type of the govening equations is changed by an elliptic one.
4. A criterion of dynamic stability of the orthotropic plate with respect to nonstationary excitations is developed: a circular orthotropic plate uniformly compressed by the radial forces $N = N^{\mathrm{crit}} = hKG_{rz}$ is under the critical state with respect to impact excitation, i.e. at $N > N^{\mathrm{crit}}$ any as small as is wished subjection of velocity to the rigid washer (the contact zone) results in its cut off with further knocking out of the plate.

Acknowledgements

The research described in this publication has been made possible in part by the Russian Foundation for Basic Research under the Grant No. 05-08-17936-a. The final part of this research has been carried out during authors' stay at Dresden Technical University as Visiting Professors through the DAAD Fellowship, which support is very much appreciated. The authors also thank the reviewers for the suggestions improving the manuscript.

References

[1] S. Abrate, Impact on laminated composite materials, *Applied Mechanics Reviews* **44** (1991), 155–190.
[2] S. Abrate, Impact on laminated composites: Recent advances, *Applied Mechanics Reviews* **47** (1994), 517–544.
[3] S. Abrate, *Impact on Laminated Composite Materials*, 2nd edition, Cambridge University Press, 2005.
[4] S.A. Ambartsumian, *Theory of Anisotropic Plates* (*Strength, Stability, and Vibrations*), Hemisphere Publishing Corporation, 1991 (English translation from the Russian edition by Nauka, Moscow, 1967).
[5] B.R. Butcher, The impact resistance of unidirectional CFRP under tensile stress, *Fibre Science and Technology* **12** (1979), 295–326.
[6] J.K. Chen and C.T. Sun, Dynamic large deflection response of composite laminates subjected to impact, *Composite Structures* **4** (1985), 59–73.
[7] J.K. Chen and C.T. Sun, Nonlinear transient responses of initially stressed composite plates, *Computers and Structures* **21** (1985), 513–520.
[8] S.T. Chiu, Y.Y. Liou, Y.C. Chang and C.L. Ong, Low velocity impact behavior of prestressed composite laminates, *Materials Chemistry and Physics* **47** (1997), 268–272.
[9] M.V. Dubinkin, Vibrations of plates with due account for rotary inertia and shear (in Russian), *Izvestija AN SSSR. Otdelenie Tekhnicheskih Nauk* **12** (1958), 131–135.
[10] R.D. Mindlin, Influence of rotary inertia and shear on flexural motions of isotropic elastic plates, *ASME Journal of Applied Mechanics* **73** (1951), 31–38.
[11] M.O. Pierson and R. Vaziri, Analytical solution for low-velocity impact response of composite plates, *AIAA Journal* **34** (1996), 1633–1640.
[12] Y. Qian and S.R. Swanson, A comparison of solution techniques for impact response of composite plates, *Composite Structures* **14** (1990), 177–192.
[13] M.D. Robb, W.S. Arnold and I.H. Marshall, The damage tolerance of GRP laminates under biaxial prestress, *Composite Structures* **32** (1995), 141–149.
[14] Yu.A. Rossikhin, On nonstationary vibrations of a plate on an elastic foundation, *Journal of Applied Mathematics and Mechanics*, **42** (1978), 347–353.
[15] Yu.A. Rossikhin and M.V. Shitikova, Nonstationary vibrations and dynamic stability of a transversely isotropic plate on an elastic isotropic half-space, in: *Structural Dynamics: Recent Advances*; Proceedings of the 5th International Conference, H.S. Ferguson, H.F. Wolfe and C. Mei, eds, Southampton, 1994, Vol. 1, pp. 130–139.
[16] Yu.A. Rossikhin and M.V. Shitikova, A ray method of solving problems connected with a shock interaction, *Acta Mechanica* **102** (1994), 103–121.
[17] Yu.A. Rossikhin and M.V. Shitikova, Non-stationary vibrations of a plate on an elastic half-space, *Journal of Sound and Vibration*, **181** (1995), 417–429.
[18] Yu.A. Rossikhin and M.V. Shitikova, Ray method for solving dynamic problems connected with propagation of wave surfaces of strong and weak discontinuities, *Applied Mechanics Reviews* **48** (1995), 1–39.
[19] Yu.A. Rossikhin and M.V. Shitikova, The ray method for solving boundary problems of wave dynamics for bodies having curvilinear anisotropy, *Acta Mechanica*, **109** (1995), 49–64.
[20] B.V. Sankar and C.T. Sun, Low-velocity impact response of laminated beams subjected to initial stresses, *AIAA Journal* **23** (1985), 1962–1969.
[21] B.V. Sankar and C.T. Sun, Low-velocity impact damage in graphite-epoxy laminates subjected to tensile initial stresses, *AIAA Journal* **24** (1986), 470–471.
[22] C.T. Sun and S. Chattopadhyay, Dynamic response of anisotropic laminated plates under initial stress to impact of a mass, *ASME Journal of Applied Mechanics* **42** (1975), 693–698.
[23] C.T. Sun and J.K. Chen, On the impact of initially stressed composite laminates, *Journal of Composite Materials* **19** (1985), 490–504.
[24] T.Y. Thomas, *Plastic Flow and Fracture in Solids*, Academic Press, New York, 1961.
[25] J.M. Whitney and N.J. Pagano, Shear deformation in heterogeneous anisotropic plates, *ASME Journal of Applied Mechanics* **37** (1970), 1031–1036.
[26] B. Whittingham, I.H. Marshall, T. Mitrevski and R. Jones, The response of composite structures with pre-stress subject to low velocity impact damage, *Composite Structures* **66** (2004), 685–698.

Appendix A

Supposing that a circular orthotropic plate experiences only flexure and shear, and transverse pressure of plate's layers is absent, the equations describing the statical behavior of such a plate possessing cylindrical anisotropy have

been written in [4] in the polar coordinate system in the following form:

$$\frac{1}{r}\,\frac{\partial(r\varphi)}{\partial r}+\frac{1}{r}\,\frac{\partial\psi}{\partial\theta}=0 \tag{A1}$$

$$\begin{aligned}&D_r\frac{\partial}{\partial r}\left(r\,\frac{\partial^2 w}{\partial r^2}\right)+D_{r\theta}\frac{\partial}{\partial r}\left(\frac{1}{r}\,\frac{\partial^2 w}{\partial\theta^2}\right)-D_\theta\left(\frac{1}{r^2}\,\frac{\partial^2 w}{\partial\theta^2}+\frac{1}{r}\,\frac{\partial w}{\partial r}\right)\\&-\frac{h^2}{10}\left\{a_r\left[D_r\frac{\partial}{\partial r}\left(r\,\frac{\partial\varphi}{\partial r}\right)+D_k\,\frac{1}{r}\,\frac{\partial^2\varphi}{\partial\theta^2}-D_\theta\,\frac{\varphi}{r}\right]\right.\\&\left.+a_\theta\left[(D_\theta\nu_r+D_k)\,\frac{\partial^2\psi}{\partial r\partial\theta}-(D_\theta+D_k)\,\frac{1}{r}\,\frac{\partial\psi}{\partial\theta}\right]\right\}+\frac{h^3}{12}\,r\varphi=0\end{aligned} \tag{A2}$$

$$\begin{aligned}&D_\theta\left(\frac{1}{r^2}\,\frac{\partial^3 w}{\partial\theta^3}+\frac{1}{r}\,\frac{\partial^3 w}{\partial r\partial\theta^2}\right)+D_{r\theta}\,\frac{\partial^3 w}{\partial r^2\partial\theta}\\&-\frac{h^2}{10}\left\{a_\theta\left[D_\theta\,\frac{1}{r}\,\frac{\partial^2\psi}{\partial\theta^2}+D_k\left(r\,\frac{\partial^2\psi}{\partial r^2}+\frac{\partial\psi}{\partial r}-\,\frac{\psi}{r}\right)\right]\right.\\&\left.+a_r\left[(D_r\nu_\theta+D_k)\,\frac{\partial^2\varphi}{\partial r\partial\theta}+(D_\theta+D_k)\,\frac{1}{r}\,\frac{\partial\varphi}{\partial\theta}\right]\right\}+\frac{h^3}{12}\,r\psi=0\end{aligned} \tag{A3}$$

where w is the plate deflection, θ is the polar angle, φ and ψ are some functions connected with the transverse forces Q_r and Q_θ, respectively, by the following formulae

$$Q_r=\frac{h^3}{12}\,\varphi,\quad Q_\theta=\frac{h^3}{12}\,\psi$$

In Eqs (A1)–(A3) the values D_r, D_θ, and C_r, C_θ are the flexure and tension rigidities in the $r-$ and $\theta-$ directions, respectively, D_k is the shear rigidity,

$$D_r=\frac{h^3}{12}\,\frac{E_r}{1-\nu_r\nu_\theta}=\frac{h^3}{12}\,B_r,\quad D_\theta=\frac{h^3}{12}\,\frac{E_\theta}{1-\nu_r\nu_\theta}=\frac{h^3}{12}\,B_\theta,\quad D_k=\frac{h^3}{12}\,B_k$$

$$D_{r\theta}=D_r\nu_\theta+2D_k,\quad a_r=G_{rz}^{-1},\quad a_\theta=G_{\theta z}^{-1},\quad B_k=G_{r\theta}$$

E_r, E_θ and $\nu_r=\nu_{\theta r}$, $\nu_\theta=\nu_{r\theta}$ are the elastic moduli and Poisson's coefficients for the r- and θ-directions, respectively, in so doing $E_r\nu_\theta=E_\theta\nu_r$, and $G_{r\theta}$, G_{rz}, and $G_{\theta z}$ are the shear moduli in the $r-\theta$, $r-z$, and $\theta-z$ planes, respectively.

For describing the dynamic behavior of the circular orthotropic plate subjected to transient loading, the set of Eqs (A1)–(A3) with formally added forces of inertia cannot be used. This is due to the fact that the dynamic system of equations written in such a manner is not the hyperbolic one. But the original idea for taking transient shear deformations and rotary inertia into account was just to change the illiptic type of plate equations for the hyperbolic one and to adapt these equations for describing wave phenomena in plates. Because of this, let us first replace the functions φ and ψ in Eqs (A1)–(A3) with

$$\varphi=\frac{12}{h^2}\,KG_{rz}\left(\frac{\partial w}{\partial r}-\,\varphi_r\right) \tag{A4}$$

$$\psi=\frac{12}{h^2}\,KG_{\theta z}\left(\frac{1}{r}\,\frac{\partial w}{\partial\theta}-\,\varphi_\theta\right) \tag{A5}$$

resulting in the known relationships for the transverse forces [10]

$$Q_r=hKG_{rz}\left(\frac{\partial w}{\partial r}-\,\varphi_r\right) \tag{A6}$$

$$Q_\theta = hKG_{\theta z}\left(\frac{1}{r}\,\frac{\partial w}{\partial \theta} - \varphi_\theta\right) \tag{A7}$$

where K is the shear coefficient which magnitude is chosen further as $5/6$, φ_r and φ_θ are the angles of rotation of the normal to the plate in the $r-$ and $\theta-$axes directions, respectively.

Substituting (A4) and (A5) into Eqs (A1)–(A3), in so doing dividing (A2) and (A3) by r, and introducing into the right-hand sides of the net equations the following forces of inertia, respectively, in Eqs through (A1) to (A3):

$$\frac{12}{h^2}\,\rho\ddot{w}, \quad \frac{h^3}{12}\,\rho\ddot{\varphi}_r, \quad \frac{h^3}{12}\,\rho\ddot{\varphi}_\theta$$

where ρ is the plate material density, yields

$$KG_{rz}\left(\frac{\partial^2 w}{\partial r^2} + \frac{1}{r}\,\frac{\partial w}{\partial r} - \frac{\partial \varphi_r}{\partial r} - \frac{1}{r}\,\varphi_r\right) + \frac{1}{r}\,KG_{\theta z}\left(\frac{1}{r}\,\frac{\partial^2 w}{\partial \theta^2} - \frac{\partial \varphi_\theta}{\partial \theta}\right) = \rho\ddot{w} \tag{A8}$$

$$\begin{aligned} &D_r\left(\frac{\partial^2 \varphi_r}{\partial r^2} + \frac{1}{r}\,\frac{\partial \varphi_r}{\partial r}\right) - D_\theta\,\frac{1}{r^2}\,\varphi_r + hKG_{rz}\left(\frac{\partial w}{\partial r} - \varphi_r\right) \\ &- (D_r\nu_\theta + D_k)\,\frac{1}{r^3}\,\frac{\partial^2 w}{\partial \theta^2} + D_k\,\frac{1}{r^2}\,\frac{\partial^2 \varphi_r}{\partial \theta^2} + (D_\theta\nu_r + D_k)\,\frac{1}{r}\,\frac{\partial^2 \varphi_\theta}{\partial r \partial \theta} \\ &- (D_\theta + D_k)\,\frac{1}{r^2}\,\frac{\partial \varphi_\theta}{\partial \theta} = \frac{\rho h^3}{12}\,\ddot{\varphi}_r \end{aligned} \tag{A9}$$

$$\begin{aligned} &D_k\left(\frac{\partial^2 \varphi_\theta}{\partial r^2} + \frac{1}{r}\,\frac{\partial \varphi_\theta}{\partial r} - \frac{1}{r^2}\,\varphi_\theta\right) + hKG_{\theta z}\left(\frac{1}{r}\,\frac{\partial w}{\partial \theta} - \varphi_\theta\right) \\ &+ D_\theta\,\frac{1}{r^2}\,\frac{\partial^2 \varphi_\theta}{\partial \theta^2} + D_\theta\,\frac{1}{r^2}\,\frac{\partial^3 w}{\partial r \partial \theta^2} - (D_\theta + 2D_k)\,\frac{1}{r^2}\,\frac{\partial^2 w}{\partial r \partial \theta} + D_k\,\frac{1}{r^3}\,\frac{\partial w}{\partial \theta} \\ &+ (D_r\nu_\theta + D_k)\,\frac{1}{r}\,\frac{\partial^2 \varphi_r}{\partial r \partial \theta} + (D_\theta + D_k)\,\frac{1}{r^2}\,\frac{\partial \varphi_r}{\partial \theta} = \frac{\rho h^3}{12}\,\ddot{\varphi}_\theta \end{aligned} \tag{A10}$$

For axially symmetric problems, the functions w and $\varphi_r = \varphi$ are independent of θ, but $\varphi_\theta = 0$, and the set of Eqs (A8)–(A10) goes over into Eqs (6) and (7) without regard for the compression force N.